Organic Communications
www.acgpubs.org
Open Access
This article is licensed under CC-BY-NC-ND 4.0
ORIGINAL ARTICLE

Design, synthesis and biological evaluation of novel *N*-napthyl-5-aryl-1,3,4-thiadiazol-2-amine derivatives as anticancer and their molecular docking studies

Prashant Rameshwarrao Yawale[1], Vivek Tukaramji Humne[2*], Nitin Lalsing Jadhao[3] and Nilesh Ramdas Thakare[4*]

[1]G. S. Tompe Arts Commerce and Science College, Chandur Bazar, Amravati, India
[2]Shri R. R. Lahoti Science College, Morshi, Amravati, India
[3]Late. N. P. W. College, Chopa, Gondia, India
[4]Shri Shivaji Science College, Amravati, India

Cite This: *Org. Commun.* 2026, 19(3), e26063946

Read Online

Abstract: A novel series of *N*-napthyl-5-aryl-1,3,4-thiadiazol-2-amine derivatives have been synthesized from naphthyl-thiosemicarbazide and carboxylic acids using intermolecular cyclization under acidic condition. The newly synthesized compounds have been characterized by IR, ^{1}H, ^{13}C NMR and mass spectral studies. All the synthesized compounds subjected to comprehensive analysis of their *in vitro* anticancer against human prostate carcinoma cell line (PC-3). Amongst, compound **3d** exhibited prominent cytotoxicity activity towards prostate cancer cell line (PC-3 cell: IC_{50} = 26.95 ± 0.06 µM), comparable to doxorubicin. Our finding provides a new structure of thiadiazole having promising potential in anticancer drug development program.

Keywords: Thiadiazole, carboxylic acid, PC-3, molecular docking

1 Introduction

Heterocyclic compound which acts as a significant framework in the development of new pharmaceuticals, represent an exceedingly important class of molecules that have attracted substantial attention in numerous biological evaluations.[1–3] The 1,3,4-thiadiazol-2-amine represent a class of five-membered heterocyclic structure containing nitrogen and sulphur atoms, that have garnered considerable attention in the field of medicinal chemistry due to their extensive range of biological activities such as anti-inflammatory[4] anticancer,[5,6] anticonvulsant,[7] antituberculosis,[8] antidiabetic,[9,10] and SARS-activity.[11] Notably, these derivatives have attracted considerable attention in the treatment of breast carcinoma, renal neoplasms, cerebral tumors, and leukemia with DNA-binding and anti-HIV activity profiles.[12] Based on the spatial arrangement of nitrogen and sulphur atom, 1,3,4-thiadiazole represent the most auspicious category concerning to antitumoral efficacy.[13–15] The incorporation of aryl substituent at the 5-position of the thiadiazole structure improved the therapeutic features, which expanding their potential in the area of cancer treatment. It is noted that the efficacy of thiadiazole derivatives which inhibiting neoplastic cell proliferation, is depend upon the specific arrangement and chemical properties of the substituents present at the aromatic ring.[16,17] In contrast, the persistence of immune activation driven by continuous toll-like receptors is a characteristic feature of various infectious, autoimmune, and malignant conditions.[18] Additionally, 5-aryl-1,3,4-thiadiazol-2-amine also open the new area of investigation to modulate the immune response, particularly through interactions with toll-like receptors (TLRs). This compound can act as ligand for TLR, and their structural modifications could enhance the ability to stimulate innate immunity. Consequently, leading to potent novel therapeutic strategies for infectious diseases and cancer treatment. As imiquimod is a well-known TLR7 agonist which demonstrated efficacy in treating skin cancers and viral infections, underscoring the therapeutic potential of TLR-targeting agents.[19] To understand the role of TLRs over all cancer cell types remains the primary challenge for clinical therapeutic application.[20,21] In order to explain significant role of thiadiazole scaffold towards anticancer therapeutic treatment, the development of such scaffold for prostate cancer is highly expectable.

*Corresponding Authors: Vivek Tukaramji Humne.
Email: vivekhumne2013@gmail.com; Nilesh Ramdas Thakare.
Email: nitinjadhao07@gmail.com, tnilesh10@gmail.com
Received: June 06, 2026
Revised: July 23, 2026
Accepted: August 01, 2026
Published: August 24, 2026

Copyright © 2026. Published by ACG Publications.

Besides, naphthyl group is also prevalent in natural products isolated from plants, microorganisms, and marine organisms. Many naphthalene-based natural compounds exhibit diverse pharmacological activities, including antifungal,[22] antioxidant,[23] anti-inflammatory,[24] and cytotoxic properties.[25] Examples of such naphthoquinones are juglone derivatives, and lapachol analogues underscore the biological relevance of naphthyl-containing scaffolds in traditional medicine and modern pharmacological research.[26] These naturally occurring compounds often serve as valuable templates for the development of new therapeutic agents and inspire synthetic modification strategies. Beyond medicinal and natural product chemistry, naphthyl groups play a significant role in materials chemistry. Their extended aromatic system contributes to strong optical absorption, fluorescence, and charge-transport properties, making them attractive building blocks for organic semiconductors, dyes, sensors, and light-emitting materials.[27] Naphthyl-based polymers and small molecules have been extensively explored in organic light-emitting diodes (OLEDs), organic photovoltaics, and molecular electronics due to their thermal stability and tunable electronic characteristics.[28] The structural rigidity of the naphthyl unit also aids in controlling molecular packing and solid-state morphology, which are critical factors in device performance. In order to study biological perspective, naphthyl compounds have been reported to interact with multiple cellular pathways, including oxidative stress modulation, enzyme inhibition, and DNA intercalation. The mechanisms in which naphthyl derivatives exerted their anticancer effects by apoptosis induction and cell cycle arrest, both of which are critical for effective cancer treatment.[29] Their planar aromatic structure pave strong interactions with biomacromolecules, which can translate into potent biological effects but may also contribute to toxicity. To the best of our knowledge, merely one report is found in the literature which has explained the potency of naphthyl-thiosemicarbazide towards prostate cell line (PC-3).[30] In consideration to aforementioned insights, we thought the incorporation of napthly-functionality at thiadiazol-2-amine could enhance the activity of anticancer against prostate cell line (PC-3).[31]

2 Experimental Detail

2.1 MTT Assay

Cytotoxicity of the provided samples on PC-3 (Procured from NCCS Pune, Passage no. 40) cell line was determined by MTT Assay. The cells (10000 cells/well) were cultured in 96 well plate for 24 h in Ham's F12k medium supplemented with 10% FBS (Fetal Bovine Serum-HIMEDIA-RM 10432) and 1% antibiotic solution (Penicillin-Streptomycin-Sigma-Aldrich P0781) at 37°C with 5% CO_2. Next day cells were treated from different concentrations of the samples (concentration as per mentioned in excel sheet). Stock solution of samples was prepared in DMSO and further diluted to get different concentrations in incomplete Cell culture Medium (Without FBS). After incubation for 24 hours, MTT Solution (5 mg/ml) was added to cell culture and further incubated (Air-jacketed CO_2 incubator-Heal force-HF90) for 2 h. Cells without treatment were considered as control and cells without MTT were considered as blank. At the end of the experiment, culture supernatant was removed, and cell layer matrix was dissolved in 100 µL dimethyl dulfoxide (DMSO–SRL-Cat no.-67685) and read in an Elisa plate reader (iMark, Biorad, USA) at 540 nM. IC_{50} was calculated by using software Graph Pad Prism-6. Images were captured under inverted microscope (Olympus ek2) using Camera (AmScope digital camera 10 MP Aptima CMOS). 50% inhibitory concentration (IC_{50}) was presented as Mean ± SEM (Standard Error of Mean).[32–34]

% Viable cells = $(A_{test}/A_{Control}) * 100$
(A_{test} = Absorbance of test sample)
($A_{Control}$ = Absorbance of Control)

2.2 Molecular Docking Study

The molecular docking simulations were performed to reveal the binding modes of synthesised compounds **3a**–**l** with prostate cell line. The structure of the estrogen receptor-ligand binding domain complex[22] was directly downloaded from the protein data bank (PDB ID 2YAT). Initially, the heteroatoms and water molecules of protein were removed, and polar hydrogens were added using Biovia Discover Studio.[35] The 2D structure of synthesized compounds were drawn and its individual structure was analysed by using Chemdraw Professional 15.0. During the optimization procedure all the parameters were set in order to obtain a stable structure with minimum energy. The docking simulation was conducted using Autodock 4.2.6 software.[36,37] The docking center was set to be the center of protein and the docking pocket size was set to be large enough to cover the whole protein molecule. The docking simulations were performed by configuring 3D grid box with center_x = −16.420870, center_y = 0.102222, −25.448593, size_x = 20, size_y = 20 and size_z = 20. The docking results were visualized using Discovery studio (Dassault Syst_emes, San Diego).[35]

2.3 General Procedure for the Synthesis of N-Napthyl-5-aryl-1,3,4-thiadiazol-2-amine (**3a–l**)

In a 15 mL Schenk tube, benzoic acid (0.1 mol) and naphyl-thiosemicarbazide (0.1 mol) in phosphorous oxychloride (5 mL) were stirred at 90°C for respective time. The completion of reaction was monitored by TLC. After the completion of reaction, the reaction mixture was poured in crushed ice followed to basified by sodium bicarbonate. The solid product was separated out and extract with ethyl acetate. The crude product was purified by column chromatography.

2.3.1 Spectral Analysis

N-(Naphthalen-1-yl)-5-phenyl-1,3,4-thiadiazol-2-amine (**3a**): White solid; 16.00 mg; Yield 67%; mp: 198–201°C; R_f: 0.2 (2:8:: EA:Pet ether); IR (ν cm^{-1}): 3685 (w), 3436 (w), 2987 (w), 2246 (w), 1768 (s), 1634 (s), 1535 (s), 1492 (s), 1034 (s), 834 (s), 787 (s), 626 (s); ^{1}H NMR (500 MHz, DMSO-d_6): δ 10.47 (br. s., 1 H), 8.21 (d, J = 7.5 Hz, 1 H), 8.29 (d, J = 8.0 Hz, 1 H), 8.06–7.90 (m, 2 H), 7.69 (t, J = 7.3 Hz, 2 H), 7.54 (m, 5 H), 7.29–7.15 (m, 1 H) ^{13}C NMR (126 MHz,

https://doi.org/10.25135/org.2606.3946
Org. Commun. 2026, 19(3):e26063946

DMSO-d_6): δ 166.5, 140.2, 134.2, 130.0, 129.5, 129.3, 128.6, 128.0, 126.8, 126.5, 126.2, 124.3, 122.3, 112.3; HRMS (ESI-qTOF) Calcd for $C_{18}H_{13}N_3S$ $[M+H]^+$, 303.0812, Found 303.3802

5-(p-tolyl)-*N*-(Naphthalen-1-yl)-1,3,4-thiadiazol-2-amine (**3b**): Brown solid; 33.0 mg; Yield 64%; mp: 133–151°C; R_f: 0.3 (2:8:: EA:Pet ether); IR (ν cm^{-1}): 3663 (w), 3443 (w), 2990 (w), 2251 (s), 2123 (s), 1771 (s), 1636 (s), 1498 (s), 1412 (s), 1233 (s), 1050 (s), 817 (s), 759 (s), 666 (s); ^{1}H NMR (500 MHz, DMSO-d_6): δ 10.38 (br. s., 1 H), 8.26 (d, *J* = 9.1 Hz, 1 H), 8.15 (d, *J* = 7.0 Hz, 1 H), 8.00–7.95 (m, 1 H), 7.73 (d, *J* = 8.0 Hz, 4 H), 7.61–7.55 (m, 3 H), 7.31 (d, *J* = 8.0 Hz, 2 H), 2.36 (s, 3 H); ^{13}C NMR (126 MHz, DMSO-d_6): δ 176.3, 152.9, 143.4, 140.0, 138.9, 133.9, 129.8, 128.3, 127.7, 126.6, 126.3, 126.0, 124.1, 122.1, 117.3, 20.9; HRMS (ESI-qTOF) Calcd for $C_{19}H_{15}N_3S$ $[M+H]^+$, 317.0514, Found 317.0615.

5-(4-Methoxyphenyl)-*N*-(naphthalen-1-yl)-1,3,4-thiadiazol-2-amine (**3c**): Brown solid; 32.0 mg; Yield 52%; mp: 135–156°C; R_f: 0.2 (2:8:: EA:Pet ether); IR (ν cm^{-1}): 3681 (w), 3506 (w), 3116 (w), 2317 (w), 1675 (s), 1607 (s), 1530 (s), 1426 (s), 1217 (s), 1034 (s), 929 (s), 844 (s), 776 (s) 627 (s); ^{1}H NMR (500 MHz, DMSO-d_6): δ 10.37 (br. s., 1 H), 8.28 (d, *J* = 7.5 Hz, 1 H), 8.15 (d, *J* = 7.5 Hz, 1 H), 7.99–7.93 (m, 1 H), 7.78 (d, *J* = 8.8 Hz, 3 H), 7.62–7.51 (m, 4 H), 7.05 (d, *J* = 8.8 Hz, 2 H), 3.81 (s, 3 H); ^{13}C NMR (126 MHz, DMSO-d_6): δ 173.1, 162.8, 157.7, 153.7, 134.0, 132.2, 131.7, 131.3, 129.6, 128.5, 128.4, 127.4, 126.4, 126.2, 126.1, 126.0, 125.9, 124.3, 123.3, 122.1, 117.6, 55.0; HRMS (ESI-qTOF) Calcd for $C_{19}H_{15}N_3OS$ $[M+H]^+$, 333.0514, Found 333.0615.

5-(2-hydroxylphenyl)-*N*-(naphthalen-1-yl)-1,3,4-thiadiazol-2-amine (**3d**): Brown solid; 20.0 mg; Yield 60%; mp: 59–78°C; R_f: 0.6 (8:2:: EA:Pet ether); IR (ν cm^{-1}): 3445(w), 3271 (w), 3069 (w), 2976 (w), 2477 (w), 2249 (w), 2119 (w), 1823 (s), 1642 (s), 1492 (s), 1334 (s), 1246 (s), 1012 (s), 819 (s), 755, 665 (s); ^{1}H NMR (500 MHz, DMSO-d_6): δ 10.97 (s, 1 H), 10.26 (br. s., 1 H), 8.32–8.25 (m, 1 H), 8.18 (d, *J* = 7.5 Hz, 1 H), 8.02 (dd, *J* = 1.6, 7.9 Hz, 1 H), 7.99–7.93 (m, 1 H), 7.71 (d, *J* = 8.1 Hz, 1 H), 7.60–7.52 (m, 4 H), 7.35–7.28 (m, 1 H), 7.04–6.93 (m, 2 H); ^{13}C NMR (126 MHz, DMSO-d_6): δ 167.3, 154.0, 136.6, 134.0, 131.1, 128.4, 127.2, 126.3, 126.1, 126.0, 123.8, 122.1, 119.8, 117.1, 117.1, 116.4; HRMS (ESI-qTOF) Calcd for $C_{18}H_{13}N_3OS$ $[M+H]^+$, 319.0614, Found 319.3315.

5-(4-Chlorophenyl)-*N*-(naphthalen-1-yl)-1,3,4-thiadiazol-2-amine (**3e**): White solid; 40.0 mg; Yield 69%; mp: 160–175°C; R_f: 0.2 (8:2:: EA:Pet ether); IR (ν cm^{-1}): 3682 (w), 3405 (w), 3020 (w), 2361 (w), 1625 (s), 1686 (s), 1527 (s), 1424 (s), 1217 (s), 1021 (s), 928 (s), 849 (s), 771 (s), 626 (s); ^{1}H NMR (400 MHz, DMSO-d_6) δ = 10.26 (br. s., 1 H), 8.32–8.24 (m, 1 H), 8.20 (d, *J* = 7.5 Hz, 1 H), 8.05–7.95 (m, 2 H), 7.71 (d, *J* = 8.1 Hz, 1 H), 7.60–7.53 (m, 3 H), 7.36–7.27 (m, 1 H), 7.04–6.93 (m, 2 H); ^{13}C NMR (126 MHz, DMSO-d_6): δ 167.8, 154.6, 137.2, 134.6, 131.7, 129.0, 127.8, 126.9, 126.7, 126.6, 126.5, 124.4, 122.7, 120.3, 117.6, 117.0 HRMS (ESI-qTOF) Calcd for $C_{18}H_{12}$ ClN_3S $[M+H]^+$, 337.0414, Found 337.8304.

5-(4-Bromophenyl)-*N*-(naphthalen-1-yl)-1,3,4-thiadiazol-2-amine (**3f**): Yellow solid; 46.5 mg; Yield 71%; mp: 128–145°C; R_f: 0.2 (8:2:: EA:Pet ether); IR (ν cm^{-1}): 3777 (w), 3686 (s), 3022 (s), 2402 (w), 1684 (s), 1524 (s), 1425 (s), 1216 (s), 1072 (s), 926 (s), 771 (s), 672 (s); ^{1}H NMR (500 MHz, DMSO-d_6): δ 10.53 (br. s., 1 H), 8.29–8.21 (m, 1 H), 8.15 (d, *J* = 7.5 Hz, 1 H), 8.00–7.95 (m, 1 H), 7.87 (d, *J* = 8.5 Hz, 1 H), 7.80 (d, *J* = 8.5 Hz, 2 H), 7.75 (d, *J* = 8.1 Hz, 1 H), 7.72–7.70 (m, 2 H), 7.61–7.57 (m, 2 H); ^{13}C NMR (126 MHz, DMSO-d_6): δ 134.6, 132.8, 132.3, 131.9, 130.3, 129.1, 129.0, 127.0, 126.8, 126.7, 126.6, 124.9, 123.9, 122.7, 118.2 HRMS (ESI-qTOF) Calcd for $C_{18}H_{12}BrN_3S$ $[M+H]^+$, 380.9914, Found 381.2815.

5-(2-Iodophenyl)-*N*-(naphthalen-1-yl)-1,3,4-thiadiazol-2-amine (**3g**): Off White solid; 68.0 mg; Yield 72%; mp: 138–158°C; R_f: 0.5 (8:2:: EA:Pet ether); IR (ν cm^{-1}): 3444(w), 2981 (w), 2475 (w), 2237 (w), 2121 (w), 1829 (s), 1645 (s), 1559 (s), 1492 (s), 1411 (s), 1240 (s), 1045 (s), 922 (s), 815 (s), 747 (s), 655 (s); ^{1}H NMR (500 MHz, DMSO-d_6): δ 10.26 (br. s., 1 H), 8.34–8.26 (m, 1 H), 8.20 (d, *J* = 7.5 Hz, 1 H), 8.05–7.95 (m, 2 H), 7.71 (d, *J* = 8.1 Hz, 1 H), 7.61–7.54 (m, 3 H), 7.36–7.29 (m, 1 H), 7.05–6.94 (m, 2 H); ^{13}C NMR (126 MHz, DMSO-d_6): δ 166.7, 153.5, 136.1, 133.5, 130.6, 127.9, 126.7, 125.8, 125.6, 125.6, 125.5, 123.3, 121.6, 119.3, 116.6, 116.0; HRMS (ESI-qTOF) Calcd for $C_{18}H_{12}I$ N_3S $[M+H]^+$, 428.9811, Found 429.2844.

5-(4-nitrophenyl)-*N*-(naphthalen-1-yl)-1,3,4-thiadiazol-2-amine (**3h**): White solid; 20.5 mg; Yield 59%; mp: 148–156°C; R_f: 0.2 (8:2:: EA:Pet ether); IR (ν cm^{-1}): 3683 (w), 3404 (w), 3019 (w), 2361 (w), 1958 (s), 1638 (s), 1580 (s), 1477 (s), 1348 (s),s 1025 (s), 928 (s), 771 (s), 670 (s), 626 (s); ^{1}H NMR (500 MHz, DMSO-d_6): δ 10.67 (br. s., 1 H), 8.31 (s, 1 H), 8.12 (s, 1 H), 7.98 (s, 5 H), 7.78 (d, *J* = 8.1 Hz, 2 H), 7.61–7.56 (m, 4 H); ^{13}C NMR (126 MHz, DMSO-d_6): δ 166.7, 153.5, 136.1, 133.5, 130.6, 127.9, 126.7, 125.8, 125.6, 125.6, 125.5, 123.3, 121.6, 119.3, 116.6, 116.0; HRMS (ESI-qTOF) Calcd for $C_{18}H_{12}N_4O_2S$ $[M+H]^+$, 348.0714, Found 348.3815.

5-(naphthalen-2-yl)-*N*-(naphthalen-1-yl)-1,3,4-thiadiazol-2-amine (**3i**): White solid; 33.0 mg; Yield 67%; mp: 198–201°C; R_f: 0.3 (9:1:: EA:Pet ether); IR (ν cm^{-1}): 3450 (w), 3068 (w), 2978 (w), 2476 (w), 2250 (w), 2121 (w), 1823 (s), 1655 (s), 1558 (s), 1491 (s), 1249 (s), 1056 (s), 820(s), 753 (s) 664 (s); ^{1}H NMR (500 MHz, DMSO-d_6): δ 10.57 (br. s., 1 H), 8.35 (s, 2 H), 8.14 (s, 2 H), 8.05–8.03 (m, 2 H), 8.00 (br. s., 2 H), 7.74 (s, 2 H), 7.60 (br. s., 4 H); ^{13}C NMR (126 MHz, DMSO-d_6): δ 168.3, 141.9, 135.7, 134.8, 134.3, 132.5, 129.4, 129.0, 128.3, 127.8, 127.3, 126.1, 124.7, 124.2, 123.5, 123.4, 122.8, 121.7, 121.2, 120.2; HRMS (ESI-qTOF) Calcd for $C_{22}H_{15}N_3S$ $[M+H]^+$, 353.1012, Found 352.4414.

5-Cyclohexyl-*N*-(naphthalen-1-yl)-1,3,4-thiadiazol-2-amine (**3j**): White solid; 59.0 mg; Yield 67%; mp: 142–163°C; R_f: 0.3 (9:1:: EA:Pet ether); IR (ν cm^{-1}): 3021 (w), 1531 (s), 1217 (s), 1025 (s), 921 (s), 765 (s), 670 (s), 671 (s); ^{1}H NMR (500 MHz, DMSO-d_6): δ 10.11 (br. s., 1 H), 8.28–8.20 (m, 1 H), 8.10 (d, *J* = 7.1 Hz, 1 H), 7.98–7.90 (m, 1 H), 7.67 (d, *J* = 8.1 Hz, 1 H), 7.58–7.54 (m, 2 H), 7.52–7.47 (m, 1 H), 2.02 (br. s., 2 H), 1.78–1.73 (m, 2 H), 1.66 (d, *J* = 12.5 Hz, 1 H), 1.53–1.27 (m, 6 H); ^{13}C NMR (126 MHz, DMSO-d_6): δ 169.9, 152.6, 143.5, 133.9, 128.3, 126.2, 126.0, 125.8, 123.5, 122.0, 116.6, 79.3, 78.9, 78.6, 32.9, 25.3; HRMS (ESI-qTOF) Calcd for $C_{18}H_{19}N_3S$ $[M+H]^+$, 309.1314, Found 309.4309.

5-(*t*-Butyl)-*N*-(naphthalen-1-yl)-1,3,4-thiadiazol-2-amine (**3k**): White solid; 63.0 mg; Yield 67%; mp: 176–195°C; R_f:

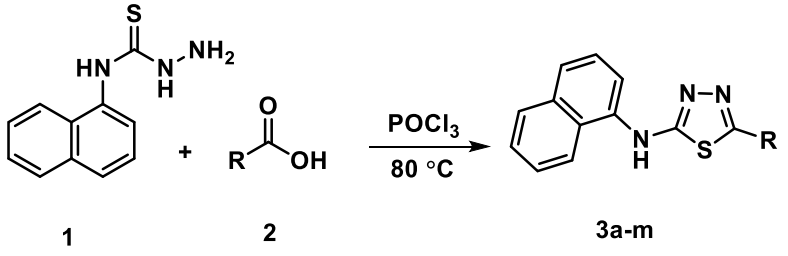
0.6 (8:2:: EA:Pet ether); IR (ν cm^{-1}): 3437 (w), 3071 (w), 2968 (w), 2512 (w), 2249 (w), 2119 (w), 1823 (s), 1662 (s), 1559 (s), 1497 (s), 1397 (s), 1220 (s), 1033 (s), 822 (s), 768 (s) 681 (s); ^{1}H NMR (500 MHz, DMSO-d_6): δ 10.17 (br. s., 1 H), 8.27–8.19 (m, 1 H), 8.05 (d, J = 7.4 Hz, 1 H), 7.98–7.91 (m, 1 H), 7.68 (d, J = 8.3 Hz, 1 H), 7.59–7.48 (m, 3 H), 1.36 (s, 9 H); ^{13}C NMR (126 MHz, DMSO-d_6): δ 167.3, 131.0, 128.3, 127.1, 126.2, 126.0, 125.9, 123.7, 122.0, 119.7, 116.9, 116.4, 34.2, 32.3; HRMS (ESI-qTOF) Calcd for $C_{16}H_{17}N_3S$ [M+H]$^+$, 283.1114, Found 283.3915.

5-styryl-*N*-(Naphthalen-1-yl)-1,3,4-thiadiazol-2-amine (**3l**): Yellow solid; 34.0 mg; Yield 65%; mp: 139–158°C; R_f: 0.2 (8:2:: EA:Pet ether); IR (ν cm^{-1}): 3404 (w), 3020 (w), 2402 (w), 1644 (s), 1542 (s), 1426 (s), 1216 (s), 1023(s), 922 (s), 764 (s), 671 (s); ^{1}H NMR (500 MHz, DMSO-d_6): δ 10.48 (br. s., 1 H), 8.25 (d, J = 8.3 Hz, 1 H), 8.10 (d, J = 7.3 Hz, 1 H), 8.00–7.94 (m, 1 H), 7.74 (d, J = 8.1 Hz, 1 H), 7.67 (d, J = 7.5 Hz, 1 H), 7.61–7.53 (m, 3 H), 7.52–7.26 (m, 5 H), 7.21 (d, J = 16.4 Hz, 1 H); ^{13}C NMR (126 MHz, DMSO-d_6): δ 135.9, 135.8, 134.2, 129.1, 129.0, 128.6, 127.3, 126.5, 126.2, 124.5, 122.3, 119.2, 118.0; HRMS (ESI-qTOF) Calcd for $C_{20}H_{15}N_3S$ [M+H]$^+$, 329.1011, Found 329.4202.

3 Results and Discussion

In continuous of our work to synthesized biological active compounds,[38–40] we started our experiment with the treatment of naphthyl-thiosemicarbazide with different carboxylic acids in phosphoric acid at 80°C to afforded *N*-napthyl-5-aryl-1,3,4-thiadiazol-2-amine as a product.[41] The reaction was neat and clean. Various substitution patterns of carboxylic acids were studied for intermolecular cyclization reaction. The time required to complete the reaction with ortho or para-substituted carboxylic acids was reduced as comparable with aliphatic carboxylic acids. However, when para-amino derivative of benzoic acid (**2m**) was used as starting material, the reaction was quenched. All the requisite products were confirmed by spectroscopic methods (Scheme 1). Further, the *in vitro* cytotoxicity of compounds **3a–l** were tested using the MTT 3-(4,5-dime thylthiazol-2-yl)-2,5-diphenyltetrazoliumbromide assay. A chemotherapy drug, doxorubicin, was used as a positive control for this study. The compounds were studied for their potencies of inhibition against prostate cancer cell. The prostate cancer cell line used in this study was PC-3 (estrogen receptor). Based on the results obtained from the MTT assay, it was observed that when the PC-3 cell line was exposed to different concentrations of the samples, cytotoxic activity was estimated for all sample and 50% inhibitory concentration as mentioned in Table 1. According to Riss,[42] a compound is regarded as an active compound if the viability of the cells after the screening test is less than 50%. Table 1 represents the IC_{50} value of the synthesized compounds **3a–l** that inhibits the growth of castration-resistant prostate cancer cells (PC-3). The compounds **3a**, **3c–3g** exhibits the greatest inhibitory effect against PC-3 compared to the other compounds in the screening test. Interestingly, compound **3d** shows highest inhibition potency (IC_{50} = 26.95 ± 0.06 µM) as comparable to doxorubicin, as a standard. This rate is influenced by cellular activity in the cytoplasm, particularly where estradiol, a type of estrogen, undergoes metabolic or functional processes. The activity of compound **3d** in this cellular context impacts PC-3 cell viability, potentially through interactions with estradiol metabolism or cytoplasmic signalling pathways. The other compounds **3a**, **3c**, **3e–3g** also showed good percentage of cell viability (IC_{50} = 35.05 ± 0.17 to 61.39 ± 0.07 µM). However, the compound **3i** have similar percentage of cell viability as doxorubicin (IC_{50} = 104.4 ± 0.18 µM). The left-over compounds **3e**, **3j–3l** showed moderate inhibition against PC-3 cell line with IC_{50} values in the range of 144.9 ± 0.10 to 659.6 ± 0.18 µM.

Based on the SAR study, the hydroxyl-functionality at ortho-position of phenyl group **(3d)** is found to be more potent against PC-3 cell line (Figure 1). The replacement of hydroxyl by iodo-functionality at ortho-position of phenyl



3a: R = Ph, 82%, 5h
3b: R = *para*-Me Ph, 87%, 5h
3c: R = *para*-MeO Ph, 89%, 5h
3d: R = *ortho*-HO Ph, 85%, 5h
3e: R = *para*-Cl Ph, 93%, 5h
3f: R = *para*-Br Ph, 90%, 5h
3g: R = *ortho*-I Ph, 89%, 5h

3h: R = *para*-NO_2 Ph,79%, 5h
3i: R = Napthyl, 88%, 5h
3j: R = cyclohexyl, 76%, 24h
3k: R = t-Butyl, 69%, 24h
3l: R = Styrene, 73%, 12h
3m:R = *para*-NH_2 Ph, 0 %,

Scheme 1. Synthesis of *N*-napthyl-5-aryl-1,3,4-thiadiazol-2-amine derivatives

https://doi.org/10.25135/org.2606.3946
Org. Commun. 2026, 19(3):e26063946

Table 1. IC_{50} values of the synthesized compounds (**3a–i**) against PC-3 cell line[a]

Compound	IC_{50} (μM)[b]
3a	55.03 ± 0.10
3b	65.13 ± 0.08
3c	53.05 ± 0.06
3d	26.95 ± 0.06
3e	291.30 ± 0.10
3f	35.05 ± 0.17
3g	61.39 ± 0.07
3h	110.25 ± 0.24
3i	104.40 ± 0.18
3j	659.60 ± 0.18
3k	263.80 ± 0.15
3l	144.90 ± 0.10
Doxorubicin	113.40 ± 0.06

Note: [a]Prostate cell line; [b]IC_{50} values (μM) are the average ± SD of three individual experiments

group **(3g)** decreased the anticancer activity. When para-position of the phenyl group was occupied by bromo-group, the potency of compound **(3f)** also increased. Including, the electron-donation group such as methoxy, and methyl group at para-position of phenyl also increase the anticancer activity (**3b** and **3c**). The introduction of naphthyl group and nitro group at the para-position of the phenyl ring (**3h** and **3i**) showed similar potency comparable to standard drug. In contrast, the aliphatic and unsaturated functionality at that position does not have prominent effect over anticancer activity study (**3j**, **3k**, and **3l**). It was also observed that the chloro-functionality at para-position of phenyl ring has no effect onto anticancer activity (**3e**).

The molecular docking studies were performed with the entire proposed series of 5-aryl-1,3,4-thiadiazol-2-amine containing napthyl; to predict the binding interaction of these compounds in the active site of estrogen receptor (Figure 2). As PC-3 cell express estrogen receptor and nowadays researchers have designed therapeutic compounds using estradiol backbone. This cell has actively recognized and grab onto these estrogen-like molecules.[43] The estrogen receptor-ligand binding domain complex PDB 2YAT has been used to study the docking pocket for anticancer screening. It was observed that thiadiazole **3b, 3d, 3f and 3i** recognized the binding pocket of enzyme correctly. These compounds formed stable key interactions with the active sites of enzymes. Including, the binding modes of substituted thiadiazole **3a–l** with estrogen receptor (PDB 2YAT) are shown in Table 2. The docking score process mainly utilized simple scoring functions which aim to gather the leading interactions. In the case of docking with 2YAT, the binding affinities of *N*-napthyl-5-aryl-1,3,4-thiadiazol-2-amine derivatives were in the order **3i** (−10.6 kcal/mol) > **3b** (−9.5 kcal/mol) > **3d = 3f** (−9.4 kcal/mol) (Table 2).

The protein-ligand complex analysis of compound **3a** demonstrates a weaker binding affinity within the series. Its interaction profile indicated interactions were stabilized by MET343 sulfur-X, LEU384 π-sigma, and π-sulfur interactions with PHE425 and HIS524. Furthermore, HIS524 provides π-π stacking, supported by numerous π-alkyl contacts with ALA350, LEU525, LEU384, LEU387, MET343, and LEU346. The compound **3b** exhibits a very strong binding affinity, indicating highly favourable thermodynamic interactions. The naphthyl group interacted with LEU384, ALA350, and LEU387 *via* the π-sigma and π-alkyl types. The presence of extensive π-alkyl contacts with ALA350, LEU525, LEU384, LEU387, ILE424, and MET343 suggests that its structural modifications allow for enhanced hydrophobic embedding within the active site. Also, the compound **3c** showed similar type of hydrophobic interactions. Mainly, hydrophobic interactions occur between different unit of compound **3d** and proteins. The naphthyl group interact with MET343, ILE424 and HIS524 with a bond length range 4.1 to 5.3°A. These interactions occur *via* π-π stacked, π-alkyl and π-alkyl. The π-π T-shaped interaction found in between phenyl ring and PHE404. The remaining hydrophobic interaction occurred *via* π-alkyl type. The docking results for compound **3e** yield a weaker affinity of −8.5 kcal/mol, revealing a binding pose essentially similar to that of **3a**. It shares the MET343 sulfur-X, LEU384 π-sigma, and corresponding π-sulfur (PHE425, HIS524) and π-π stacking (HIS524) interactions. The redundant π-alkyl contacts (ALA350, LEU525, LEU384, LEU387, MET343, LEU346) suggest that the structural differences in **3e** do not impart any additional thermodynamic interactions over **3a**. The compound **3f** displayed a very strong binding profile, closely mirroring the high efficacy of compound **3b**. Interactions such as LEU384 π-sigma, PHE425 π-sulfur, and HIS524 π-π stacking are prominent in this compound. The

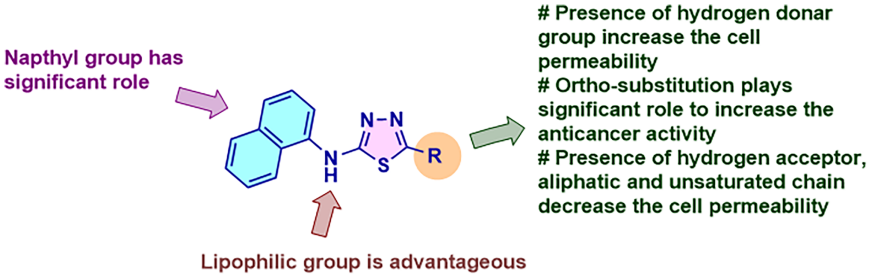


Figure 1. Structure activity relationship study

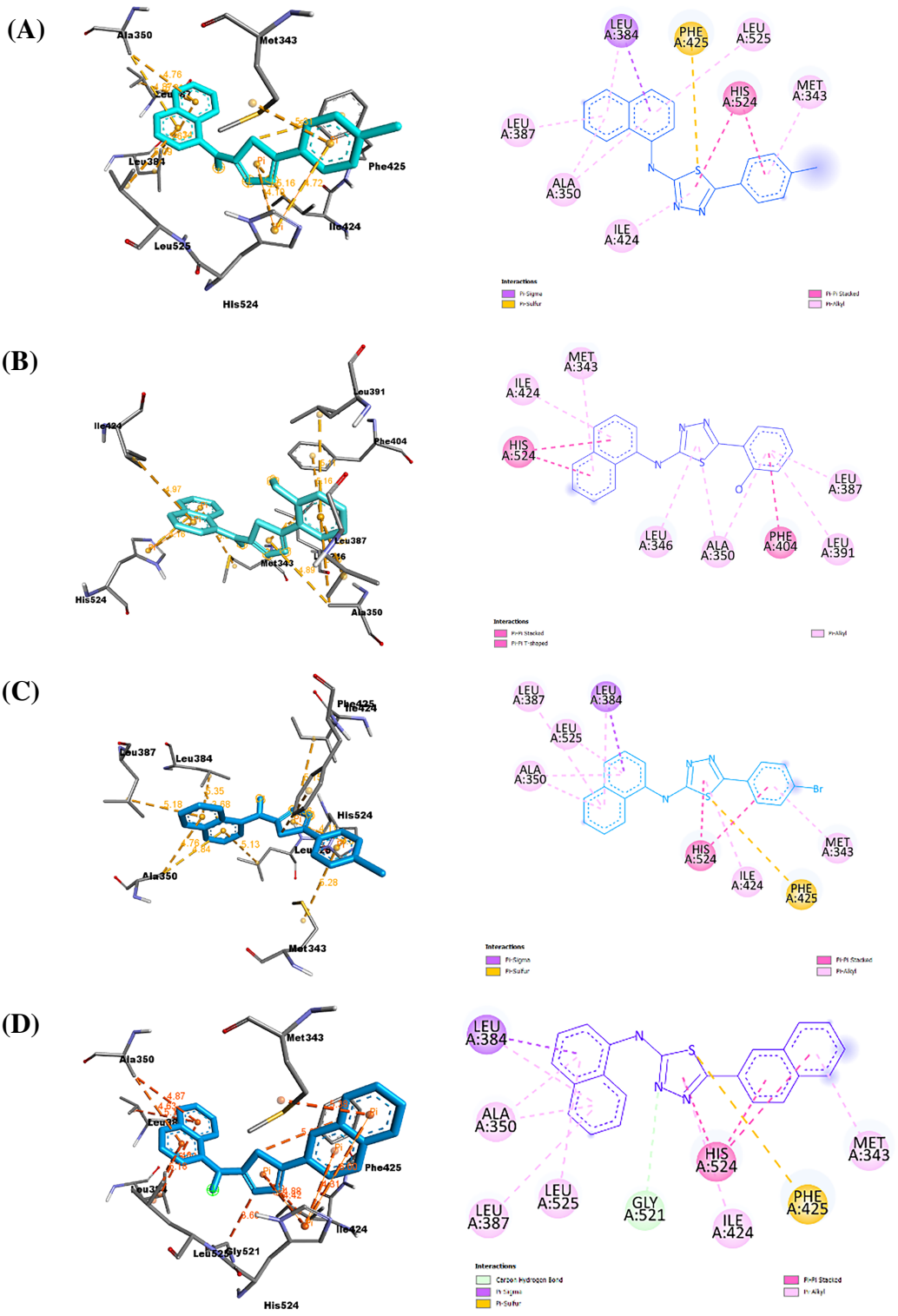


Figure 2. Binding interaction of (A) compound **3b**, (B) compound **3d** (C) compound **3f** (D) compound **3i** with prostate cancer cells (PDB 2YAT)

repeated π-alkyl contacts with ALA350, LEU525, LEU384, LEU387, ILE424, and MET343 indicated a highly complementary geometry that effectively exploits the hydrophobic nature of the receptor pocket. Despite being one of the weakest binders, compound **3g** presents a unique interaction paradigm, notably a π-donor hydrogen bond with HIS524. It has observed the presence of iodo-fuctionality makes the π-alkyl (hydrophobic) interaction with thiadiazole with bond length 4.1°A. In compound **3h**, the binding is mediated by HIS524 π-π stacking and a PHE404 π-π T-shaped interaction. Furthermore, a varied array of π-alkyl contacts with LEU387, MET388, LEU391, LEU349, ALA350,

https://doi.org/10.25135/org.2606.3946
Org. Commun. 2026, 19(3):e26063946

and MET343 indicates that the molecule efficiently occupies the distal hydrophobic sub-pockets. In compound **3i**, the hydrogen interaction has been observed between thiadiazole unit and GLY521 with bond length 3.6°A. The *N*-napthyl group interact with different protein unit *viz.* ALA350, LEU525, ALA350, LEU384, LEU387 *via* π-alkyl and π-sigma hydrophobic interaction. The bond length was found to be in the range of 4.6 to 5.1°A for such hydrophobic interaction. The other naphthyl group of **3i** formed π-π stacked hydrophobic interaction with HIS524 of bond lengths of 4.3 and 5.3°A respectively. The other type of hydrobhobic interaction occur between PHE425 *via* π-sulphur type (bond length: 5.6°A). However, the multiplicity of its π-alkyl contacts (ALA350, LEU525, LEU384, LEU387, ILE424, MET343) implies maximum desolvation and optimal Vander-waals contacts. The compound **3j** indicates strong predictive interactions include LEU384 (π-sigma), PHE425 (π-sulfur), HIS524 (π-π) stacked, and PHE404 π-π T-shaped configurations. The broad hydrophobic contacts with MET343, PHE425, HIS524, ALA350, LEU384, MET388, and ILE424 suggest a versatile accommodation of the ligand's structural framework. The compound **3k** exhibits a moderate-to-weak binding affinity of −8.6 kcal/mol. The molecule is localized *via* a PHE404 π-π T-shape interaction, pure alkyl contacts with MET343 and LEU525, and various π-alkyl interactions involving HIS524, LEU387, MET388, LEU391, LEU349, ALA350, and LEU384. Notably, the specific contact annotated as 'Methyl-Thiadiazole' indicating a distinct

Table 2. The interactions available on molecular docking analysis of synthesized compounds with Estrogen receptor (2YAT)

Compounds	Binding affinity (kcal/mol)	Receptor	Type of interactions	Distance (Å)
3a	−8.5	MET343	Sulfur-X (Other)	3.3
		LEU384	π-Sigma (Hydrophobic)	3.6
		PHE425	π-Sulfur (Other)	5.3
		HIS524	π-Sulfur (Other)	4.3
		HIS524	π-π Stacked (Hydrophobic)	4.8, 4.3
		ALA350	π-Alkyl (Hydrophobic)	4.5
		LEU525	π-Alkyl (Hydrophobic)	5.2
		ALA350	π-Alkyl (Hydrophobic)	4.7
		LEU384	π-Alkyl (Hydrophobic)	5.3
		LEU387	π-Alkyl (Hydrophobic)	5.0
		MET343	π-Alkyl (Hydrophobic)	5.2
		LEU346	π-Alkyl (Hydrophobic)	5.3
3b	−9.5	LEU384	π-Sigma (Hydrophobic)	3.6
		PHE425	π-Sulfur (Other)	5.3
		HIS524	π-π Stacked (Hydrophobic)	4.0, 4.7
		ALA350	π-Alkyl (Hydrophobic)	4.8
		LEU525	π-Alkyl (Hydrophobic)	5.0
		ALA350	π-Alkyl (Hydrophobic)	4.7
		LEU384	π-Alkyl (Hydrophobic)	5.3
		LEU387	π-Alkyl (Hydrophobic)	5.2
		ILE424	π-Alkyl (Hydrophobic)	5.1
		MET343	π-Alkyl (Hydrophobic)	5.3
3c	−9.0	PHE425	π-Sulfur (Other)	5.3
		HIS524	π-π Stacked (Hydrophobic)	4.1
		MET343	Alkyl (Hydrophobic)	5.2
		PHE425	π-Alkyl (Hydrophobic)	4.3
		HIS524	π-Alkyl (Hydrophobic)	4.6
		ILE424	π-Alkyl (Hydrophobic)	5.1
3d	−9.4	HIS524	π-π Stacked (Hydrophobic)	4.1
		PHE404	π-π T Shaped (Hydrophobic)	5.1
		ILE424	π-Alkyl (Hydrophobic)	4.9
		MET343	π-Alkyl (Hydrophobic)	5.3
		LEU346	π-Alkyl (Hydrophobic)	4.5
		ALA350	π-Alkyl (Hydrophobic)	4.8, 4.9
		LEU387	π-Alkyl (Hydrophobic)	4.2
		LEU391	π-Alkyl (Hydrophobic)	5.1

Table 2. (Continued)

Compounds	Binding affinity (kcal/mol)	Receptor	Type of interactions	Distance (Å)
3e	−8.5	MET343:	Sulphur-X (Other)	3.3
		LEU384	π-σ (Hydrophobic)	3.6
		PHE425	π-Sulfur (Other)	5.3
		HIS524	π-Sulfur (Other)	4.3
		HIS524	π-π Stacked (Hydrophobic)	4.8, 4.2
		ALA350	π-Alkyl (Hydrophobic)	4.5
		LEU525	π-Alkyl (Hydrophobic)	5.2
		ALA350	π-Alkyl (Hydrophobic)	4.7
		LEU384	π-Alkyl (Hydrophobic)	5.3
		LEU387	π-Alkyl (Hydrophobic)	5.0
		MET343	π-Alkyl (Hydrophobic)	5.2
		LEU346	π-Alkyl (Hydrophobic)	5.3
3f	−9.4	LEU384	π-σ (Hydrophobic)	3.6
		PHE425	π-Sulfur (Other)	5.3
		HIS524	π-π Stacked (Hydrophobic)	4.1, 4.6
		ALA350	π-Alkyl (Hydrophobic)	4.8, 4.7
		LEU525	π-Alkyl (Hydrophobic)	5.1
		LEU384	π-Alkyl (Hydrophobic)	5.3, 3.6
		LEU387	π-Alkyl (Hydrophobic)	5.1
		ILE424	π-Alkyl (Hydrophobic)	5.1
		MET343	π-Alkyl (Hydrophobic)	5.2
3g	−8.5	HIS524	π-Donar (Hydrogen Bond)	3.0
		LEU384	π-σ (Hydrophobic)	3.8
		MET343	π-Sulfur (Other)	4.7
		PHE425	π-π Stacked (Hydrophobic)	4.0
		PHE425	π-π Stacked (Hydrophobic)	4.2
		HIS524	π-π Stacked (Hydrophobic)	4.6
		LEU346	Alkyl (Hydrophobic)	4.2
		PHE404	π-Alkyl (Hydrophobic)	5.0
		ALA350	π-Alkyl (Hydrophobic)	4.8
		LEU525	π-Alkyl (Hydrophobic)	4.6
		Iodo-Thiadiazole	π-Alkyl (Hydrophobic)	4.1
3h	−9.3	HIS524	π-π Stacked (Hydrophobic)	4.1
		PHE404	π-π T Shaped (Hydrophobic)	4.8
		LEU387	π-Alkyl (Hydrophobic)	4.5
		MET388	π-Alkyl (Hydrophobic)	5.2
		LEU391	π-Alkyl (Hydrophobic)	5.0
		LEU349	π-Alkyl (Hydrophobic)	5.2
		ALA350	π-Alkyl (Hydrophobic)	4.5
		LEU387	π-Alkyl (Hydrophobic)	4.7
		LEU391	π-Alkyl (Hydrophobic)	5.4
		MET343	π-Alkyl (Hydrophobic)	5.4
3i	−10.6	GLY521	Carbon-Hydrogen (Hydrogen bond)	3.6
		LEU384	π-σ (Hydrophobic)	3.4
		PHE425	π-Sulfur (Other)	5.6
		HIS524	π-π Stacked (Hydrophobic)	4.4, 4.3, 5.9
		ALA350	π-Alkyl (Hydrophobic)	4.6, 4.8
		LEU525	π-Alkyl (Hydrophobic)	5.1
		LEU384	π-Alkyl (Hydrophobic)	5.2
		LEU387	π-Alkyl (Hydrophobic)	5.1
		ILE424	π-Alkyl (Hydrophobic)	4.8
		MET343	π-Alkyl (Hydrophobic)	5.3

https://doi.org/10.25135/org.2606.3946
Org. Commun. 2026, 19(3):e26063946

Table 2. (Continued)

Compounds	Binding affinity (kcal/mol)	Receptor	Type of interactions	Distance (Å)
3j	−9.3	LEU384	π-σ (Hydrophobic)	3.5
		PHE425	π-Sulfur (Other)	5.3
		HIS524	π-π Stacked (Hydrophobic)	4.3
		PHE404	π-π T Shaped (Hydrophobic)	5.6
		MET343	Alkyl (Hydrophobic)	5.4
		PHE425	π-Alkyl (Hydrophobic)	4.2
		HIS524	π-Alkyl (Hydrophobic)	4.6
		ALA350	π-Alkyl (Hydrophobic)	4.8
		LEU384	π-Alkyl (Hydrophobic)	5.3
		MET388	π-Alkyl (Hydrophobic)	4.5
		ILE424	π-Alkyl (Hydrophobic)	5.1
3k	−8.6	PHE404	π-π T Shape (Hydrophobic)	4.8
		MET343	Alkyl (Hydrophobic)	5.0, 4.9
		LEU525	Alkyl (Hydrophobic)	3.9
		HIS524	π-Alkyl (Hydrophobic)	4.1, 4.3
		LEU387	π-Alkyl (Hydrophobic)	4.4
		MET388	π-Alkyl (Hydrophobic)	5.2
		LEU391	π-Alkyl (Hydrophobic)	4.8
		LEU349	π-Alkyl (Hydrophobic)	5.1
		ALA350	π-Alkyl (Hydrophobic)	4.5
		LEU387	π-Alkyl (Hydrophobic)	4.7
		LEU384	π-Alkyl (Hydrophobic)	5.3
		LEU525	π-Alkyl (Hydrophobic)	5.2
		Methyl-Thiadiazole	π-Alkyl (Hydrophobic)	3.3,3.4, 3.5
3l	−9.0	MET388	π-Sulfur (Other)	5.66252
		PHE425	π-Sulfur (Other)	5.59446
		HIS524	π-π Stacked (Hydrophobic)	4.44105
		PHE404	π-π T Shaped (Hydrophobic)	5.43948
		PHE404	π-π T Shaped (Hydrophobic)	4.89287
		MET343	Alkyl (Hydrophobic)	4.92751
		LEU346	Alkyl (Hydrophobic)	4.95279
		PHE425	π-Alkyl (Hydrophobic)	4.78964
		LEU387	π-Alkyl (Hydrophobic)	5.00269
		LEU391	π-Alkyl (Hydrophobic)	5.171
		ALA350	π-Alkyl (Hydrophobic)	4.80582
		LEU387	π-Alkyl (Hydrophobic)	4.56258
		LEU391	π-Alkyl (Hydrophobic)	5.23433
		LEU346	π-Alkyl (Hydrophobic)	5.19426

moiety-directed interaction. The compound **3l** demonstrates a robust interaction profile with a moderate-strong score of −9.0 kcal/mol. It is primarily stabilized by dual π-sulphur contacts with MET388 and PHE425, HIS524 π-π stacking, and notably two distinct PHE404 π-π T-shaped interactions. Alkyl and π-alkyl contacts with MET343, LEU346, PHE425, LEU387, LEU391, and ALA350 further confirm its secure pocket within the receptor cavity.

4 Conclusion

In conclusion, the findings of this study indicate that the *N*-napthyl-5-aryl-1,3,4-thiadiazol-2-amine derivative **3d** where the hydroxyl group situated at ortho-position showed prominent anticancer effect against PC-3 comparable to the standard drug; doxorubicin. The molecular docking study was conducted to explained the desired thiadiazol-2-amine derivative's binding affinity and thermodynamical interactions. The present molecular docking studies showed that compound **3b**, **3d**, **3f**, and **3i** with para methyl and chloro group and ortho-substituted hydroxyl group at phenyl group have good binding affinity with estrogen receptor. However, the anticancer and molecular docking studies are good agreed with compound **3d**. Thus, integrating pharmacokinetic and molecular docking analysis verifies in vitro findings and enhances the potential of these compounds in medicinal applications.

Acknowledgement

Authors thankful to G. S. Tompe Arts Commerce and Science College, Chandur Bazar, India to provide necessary facilities Authors also thankful to Department of Chemistry, Savitribai Phule Pune University for providing characterization data.

Author Contributions

Nilesh Ramdas Thakare (NRT) and Vivek Tukaramji Humne (VTH) conceptualized and designed the research. Prashant Rameshwarrao Yawale (PRY) and Nitin Lalsing Jadhao (NLJ) performed the experiments and anticancer study. VTH and NLJ analysed and interpreted the data. PRY and NLJ prepared the original draft of the manuscript, and VTH critically revised it. All authors have read and approved the final version of the manuscript.

Availability of Data and Materials

The authors declare that the data supporting the findings of this study are available within the paper and its Supplementary Information files. Should any raw data files be needed in another format they are available from the corresponding author upon reasonable request. Source data are provided with this paper.

Ethics Approval

Ethical approval was not required for this study as it was conducted entirely in vitro using established, commercially available human cancer cell lines (PC-3) procured from NCCS Pune, India. The study did not involve any human participants, primary tissue samples, or animal subjects.

Artificial Intelligence (AI) Statement

The authors affirm that no Artificial Intelligence (AI) tools were employed in the preparation of this manuscript, which includes language editing, graphical abstract preparation, figure generation, or image editing.

Conflicts of Interest

The authors declare that they do not have any conflict of interest.

Supporting Information

Supporting information accompanies this paper on http://www.acgpubs.org/journals/organic-communications.

ORCID

Prashant Rameshwarrao Yawale: 0009-0000-9224-2821
Vivek Tukaramji Humne: 0000-0002-3412-5149
Nitin Lalsing Jadhao: 0009-0002-5451-5942
Nilesh Ramdas Thakare: 0000-0002-4501-2254

References

[1] Yang, S. -J., Lee, S-H., Kwak, H-J. & Gong, Y-D. (2013). Regioselective synthesis of 2-amino-substituted 1, 3, 4-oxadiazole and 1, 3, 4-thiadiazole derivatives via reagent-based cyclization of thiosemicarbazide intermediate. *The Journal of Organic Chemistry*, *78*(2), 438–444. DOI: 10.1021/jo302324r.

[2] Rakesh, K. P., Shantharam, C. S., Sridhara, M. B., Manukumar, H. M. & Qin, H. -L. (2017). Benzisoxazole: A privileged scaffold for medicinal chemistry. *MedChemComm*, *8*(11), 2023–2039. DOI: 10.1039/c7md00449d.

[3] Hawash, M., Jaradat, N., Abualhasan, M., Amer, J., Levent, S., Issa, S., Ibrahim, S., Ayaseh, A., Shtayeh, T. & Mousa, A. (2021). Synthesis, chemo-informatics, and anticancer evaluation of fluorophenyl-isoxazole derivatives. *Open Chemistry*, *19*(1), 855–863. DOI: 10.1515/chem-2021-0078.

[4] Mehta, D. K., Taya, P., Das, R. & Dua, K. (2019). Design, synthesis and molecular docking studies of novel thiadiazole analogues with potential antimicrobial and anti-inflammatory activities. *Anti-Inflammatory & Anti-Allergy Agents in Medicinal Chemistry*, *18*(2), 91–109. DOI: 10.2174/1871520619666190307162442.

[5] Janowska, S., Paneth, A. & Wujec, M. (2020). Cytotoxic properties of 1, 3, 4-thiadiazole derivatives—a review. *Molecules*, *25*(18), 4309. DOI: 10.3390/molecules25184309.

[6] Charitos, G., Trafalis, D. T., Dalezis, P., Potamitis, C., Sarli, V. & Zoumpoulakis, P. (2019). Synthesis and anticancer activity of novel 3, 6-disubstituted 1, 2, 4-triazolo-[3, 4-b]-1, 3, 4-thiadiazole derivatives. *Arabian Journal of Chemistry*, *12*(8), 4784–4794. DOI: 10.1016/j.arabjc.2016.09.015.

[7] Luszczki, J. J., Karpińska, M., Matysiak, J. & Niewiadomy, A. (2015). Characterization and preliminary anticonvulsant assessment of some 1, 3, 4-thiadiazole derivatives. *Pharmacological Reports*, *67*(3), 588–592. DOI: 10.1016/j.pharep.2014.12.008.

[8] Sekhar, D., Venkata Rao, D. V., Rao, A. T., Kumar, U. V. & Jha, A. (2019). Design and synthesis of 1,3,4-thiadiazole derivatives as novel anticancer and antitubercular agents. *Russian Journal of General Chemistry*, *89*(4), 770–779. DOI: 10.1134/S1070363219040224.

[9] Vaishnav, Y., Dewangan, D., Verma, S., Mishra, A., Thakur, A. S. & Kashyap, P. (2020). PPAR gamma targeted molecular docking and synthesis of some new amide and urea substituted 1, 3, 4-thiadiazole derivative as antidiabetic compound. *Journal of Heterocyclic Chemistry*, *57*(5), 2213–2224. DOI: 10.1002/jhet.3941.

[10] Hameed, S., Varkey, J. & Jayasekhar, P. (2020). In Silico design, synthesis and in vitro antidiabetic activity of novel 5-furyl-1, 3, 4-thiadiazolimines. *International Journal of Pharma Sciences and Research*, *11*(6), 152–159. DOI: 10.21817/ijpsr/2020/v11i6/201106011.

[11] Messore, A., Malune, P., Patacchini, E., Madia, V. N., Ialongo, D., Arpacioglu, M., Albano, A., Ruggieri, G., Saccoliti, F., Scipione, L., Tramontano, E., Canton, S., Corona, A., Scognamiglio, S., Paulis, A., Suleiman, M., Mohammed Al-Maqtari, H., Abid, F. M. A., Kawsar, S. M. A., Sankaranarayanan, M. et al. (2024). New thiazolidine-4-one derivatives as SARS-CoV-2 main protease inhibitors. *Pharmaceuticals*, *17*(5), 650. DOI: 10.3390/ph17050650.

[12] Kumar, V., Dey, S., Saha, S. & Chakraborty, S. (2023). Molecular docking and dynamics simulation of natural compounds against SARS-CoV-2 main protease. *Journal of Biomolecular*

Structure and Dynamics, *41*(10), 2413–2426. DOI: 10.1080/07391102.2023.2226713.

[13] Ahmed, S., Bhat, A. R., Rahiman, A. K., Dongre, R. S., Hasan, A., Niranjan, V. C. L., Sheikh, S. A., Jamalis, J., Berredjem, M. & Kawsar, S. M. A. (2024). Green synthesis, antibacterial and antifungal evaluation of new thiazolidine-2,4-dione derivatives: Molecular dynamic simulation, POM study and identification of antitumor pharmacophore sites. *Journal of Biomolecular Structure & Dynamics*, *42*(20) 10635–10651. DOI: 10.1080/07391102.2023.2258404.

[14] Kumar, D., Kumar, H., Kumar, V., Deep, A., Sharma, A., Marwaha, M. G. & Marwaha, R. K. (2023). Mechanism-based approaches of 1,3,4 thiadiazole scaffolds as potent enzyme inhibitors for cytotoxicity and antiviral activity. *Medicine in Drug Discovery*, *17*(17), 100150. DOI: 10.1016/j.medidd.2022.100150.

[15] Janowska, S., Khylyuk, D., Bielawska, A., Szymanowska, A., Gornowicz, A., Bielawski, K., Noworól, J., Mandziuk, S. & Wujec, M. (2022). New 1,3,4-thiadiazole derivatives with anticancer activity. *Molecules*, *27*(6), 1814. DOI: 10.3390/molecules27061814.

[16] Kokovina, T. S., Gadomsky, S. Y., Terentiev, A. A. & Sanina, N. A. (2021). A novel approach to the synthesis of 1,3,4-thiadiazole-2-amine derivatives. *Molecules*, *26*(17), 5159. DOI: 10.3390/molecules26175159.

[17] Yang, X. -H., Xiang, L., Li, X., Zhao, T. -T., Zhang, H., Zhou, W. -P., Wang, X. -M., Gong, H. -B. & Zhu, H. -L. (2012). Synthesis, biological evaluation, and molecular docking studies of 1,3,4-thiadiazol-2-amide derivatives as novel anticancer agents. *Bioorganic and Medicinal Chemistry*, *20*(9), 2789–2795. DOI: 10.1016/j.bmc.2012.03.040.

[18] Patinote, C., Bou Karroum, N., Moarbess, G., Cirnat, N., Kassab, I., Bonnet, P.-A. & Deleuze-Masquéfa, C. (2020). Agonist and antagonist ligands of toll-like receptors 7 and 8: Ingenious tools for therapeutic purposes. *European Journal of Medicinal Chemistry*, *193*(Suppl 1), 112238. DOI: 10.1016/J.EJMECH.2020.112238.

[19] Kaushik, D., Kaur, A., Petrovsky, N. & Salunke, D. B. (2021). Structural evolution of toll-like receptor 7/8 agonists from imidazoquinolines to imidazoles. *RSC Medicinal Chemistry*, *12*(7), 1065–1120. DOI: 10.1039/D1MD00031D.

[20] Kundu, S., Lee, C., Billips, B. K., Habermacher, G. M., Zhang, Q., Liu, V., Wong, L., Klumpp, D. J. & Thumbikat, P. (2008). The toll-like receptor pathway: A novel mechanism of infection-induced carcinogenesis of prostate epithelial cells. *The Prostate*, *68*(2), 223–229. DOI: 10.1002/PROS.20710.

[21] Kaur, A., Kaushik, D., Piplani, S., Mehta, S. K., Petrovsky, N. & Salunke, D. B. (2021). TLR2 agonistic small molecules: Detailed structure-activity relationship, applications, and future prospects. *Journal of Medicinal Chemistry*, *64*(1), 233–278. DOI: 10.1021/ACS.JMEDCHEM.0C01627.

[22] Altintop, M. D., Atli, O., Ilgin, S., Demirel, R., Özdemir, A. & Kaplancıklı, Z. A. (2016). Synthesis and biological evaluation of new naphthalene substituted thiosemicarbazone derivatives as potent antifungal and anticancer agents. *Europian Journal of Medicinal Chemistry*, *108*(5), 406–414. DOI: 10.1016/j.ejmech.2015.11.041.

[23] Ateş-Alagöz, Z., Kuş, C. & Coban, T. (2005). Synthesis and antioxidant properties of novel benzimidazoles containing substituted indole or 1,1,4,4-tetramethyl-1,2,3,4-tetrahydronaphthalene fragments. *Journal of Enzyme Inhibition and Medicinal Chemistry*, *20*(4), 325–331. DOI: 10.1080/14756360500131706.

[24] Voskienė, A., Sapijanskaitė, B., Mickevičius, V., Jonuškienė, I., Stasevych, M., Komarovska-Porokhnyavets, O., Musyanovych, R. & Novikov, V. (2012). Synthesis and microbiological evaluation of new 2- and 2,3-diphenoxysubstituted naphthalene-1,4-diones with 5-oxopyrrolidine moieties. *Molecules*, *17*(12), 14434–14448. DOI: 10.3390/molecules171214434.

[25] Meier, C., Steinhauer, T. N., Koczian, F., Plitzko, B., Jarolim, K., Girreser, U., Braig, S., Marko, D. & Vollmar, A. M. (2017). A dual topoisomerase inhibitor of intense pro-apoptotic and antileukemic nature for cancer treatment. *ChemMedChem*, *12*(5), 347–352. DOI: 10.1002/cmdc.201700026.

[26] Juang, Y. -P., Tsai, J. -Y., Gu, W. -L., Hsu, H. -C., Lin, C. -L., Wu, C. -C. & Liang, P. -H. (2024). Discovery of 5-hydroxy-1,4-naphthoquinone (Juglone), 2024 derivatives as dual effective agents targeting platelet-cancer interplay through protein disulfide isomerase inhibition. *Journal of Medicinal Chemistry*, *67*(5), 3626–3642. DOI: 10.1021/acs.jmedchem.3c02107.

[27] Rana, P., Siva, M., Lo, R. & Das, P. (2024). A naphthalene–phenanthro[9,10-d]imidazolebased p-conjugated molecule with a self-assembly-induced tuneable multiple fluorescence output exhibits artificial light-harvesting properties. *Material Advance*, *5*, 8208. DOI: 10.1039/d4ma00806e.

[28] Qiu, X., Liu, X., Ji, Y., Ma, C., Li, J., Liu, X., Zhou, J. & Xue, S. (2024). An acridine and naphthalene-fused chromophore for Rec. 2020 standard deep-blue OLEDs with high color purity and low-efficiency roll-off. *Organic Chemistry Frontiers*, *11*(24), 7136–7146. DOI: 10.1039/D4QO01751J.

[29] Luo, L., Jia, J. J., Zhong, Q., Zhong, X., Zheng, S., Wang, G. & He, L. (2021). Synthesis and anticancer activity evaluation of naphthalene-substituted triazole spirodienones. *European Journal of Medicinal Chemistry*, *213*, 113039. DOI: 10.1016/J.EJMECH.2020.113039.

[30] Anisree, S., Shanmugavelan, P., Palanisamy, S., Kishore, R. & Srivastava, N. (2024). Synthesis and anticancer screening of substituted (phenyl)-1-((naphthalen-5-yl)methylene) thiosemicarbazide against PC3 prostate cancer cells. *Journal of the Indian Chemical Society*, *101*(9), 101229. DOI: 10.1016/j.jics.2024.101229.

[31] Kamalidehghan, B., Ghafouri-Fard, S., Motevaseli, E. & Ahmadipour, F. (2018). Inhibition of human prostate cancer (PC-3) cells and targeting of PC-3-derived prostate cancer stem cells with koenimbin, a natural dietary compound from Murraya koenigii (l) spreng. *Drug Design, Development and Therapy*, *12*, 1119–1133. DOI: 10.2147/DDDT.S156826.

[32] Humne, V. T., Birhade, D. R. & Pawar, O. B. (2025). Ionic-liquid-mediated one-pot synthesis of novel 2-pyrazole-*N*-thiazole-thiazolidinone hybrid as COX-1/COX-2 inhibitor. *Organic Communication*, *18*(3), 153–165. DOI: 10.25135/acg.oc.193.2506.3564.

[33] Jadhao, N. L., Musale, H. B., Gajbhiye, J. M. & Humne, V. T. (2024). Copper-mediated [3+2] oxidative cyclization of oxime acetate and their utility in formal synthesis of fentiazac. *Organic and Biomolecular Chemistry*, *22*(3), 521–528. DOI: 10.1039/D3OB01882B.

[34] Gayake, R. A., Jagrut, V. B. & Humne, V. T. (2022). Efficient one-pot cascade synthesis of pyrazolopyridazine in PEG-400. *Organic Communication*, *15*(3), 297–303. DOI: 10.25135/acg.oc.135.2204.2408.

[35] Keerthi Kumar, C. T., Keshavayya, J., Rajesh, T. N., Peethambar, S. K. & Shoukat Ali, A. R. (2013). Synthesis, characterization, and biological activity of 5-phenyl-1,3,4-thiadiazole-2-amine incorporated azo dye derivatives. *Organic Chemistry International*, *2013*, 370626. DOI: 10.1155/2013/370626.

[36] Riss, T. L., Moravec, R. A., Niles, A. L., Duellman, S., Benink, H. A., Worzella, T. J., Minor, L. (2004). Cell viability assays. *Assay Guidance Manual, Bethesda (MD): Eli Lilly & Company and the National Center for Advancing Translational Sciences*.

[37] Tai, S., Sun, Y., Squires, J., Zhang, H., Zhang, H., Oh, W., Liang, C. & Huang, J. (2011). PC3 is a cell line characteristic of prostatic small cell carcinoma. *The Prostate*, *71*(15), 1668–1679. DOI: 10.1002/PROS.21383.

[38] Morgan, D. M. (1998). Tetrazolium (MTT) assay for cellular viability and activity. *Methods in Molecular Biology*, *79*, 179–184. DOI: 10.1385/0-89603-448-8:179.

[39] Van Meerloo, J., Kaspers, G. J. L. & Cloos, J. (2011). Cell sensitivity assays: The MTT assay. *Methods in Molecular Biology*, *731*, 237–245. DOI: 10.1007/978-1-61779-080-5_20.

[40] Fotakis, G. & Timbrell, J. A. (2006). *In vitro* cytotoxicity assays: Comparison of LDH, neutral red, MTT and protein assay in hepatoma cell lines following exposure to cadmium chloride. *Toxicology Letters*, *160*, 171–177. DOI: 10.1016/j.toxlet.2005.07.001.

[41] More, R. M., Jakkawad, A. L., Kadam, A. B., Musale, H. B., Humne, V. T. & Junne, S. B. (2024). Design and synthesis of novel thiazolidinone hybrid as α-amylase inhibitor, glucose uptake and antioxidant activity. *Results in Chemistry*, *9*, 101657. DOI: 10.1016/j.rechem.2024.101657.

[42] Morris, G. M., Goodsell, D. S., Halliday, R. S., Huey, R., Hart, W. E., Belew, R. K. & Olson, A. J. (1998). Automated docking using a Lamarckian genetic algorithm and an empirical binding free energy function. *Journal of Computational Chemistry*, *19*, 1639–1662. DOI: 10.1002/(SICI)1096-987X(19981115)19:14<1639::AID-JCC10>3.0.CO;2-B.

[43] Trott, O. & Olson, A. J. (2010). AutoDock Vina: Improving the speed and accuracy of docking with a new scoring function, efficient optimization, and multithreading. *Journal of Computational Chemistry*, *31*(2), 455–461. DOI: 10.1002/jcc.21334.